

## FORMATION AND MORPHOLOGY OF COLLOIDAL CHITOSAN-STABILIZED COPPER SULFIDES

H.T. Boey, W.L. Tan, N.H.H. Abu Bakar, M. Abu Bakar\* and J. Ismail

Nanoscience Research Laboratory  
School of Chemical Sciences, Universiti Sains Malaysia  
11800 USM, Pulau Pinang, Malaysia

\*Corresponding author: bmohamad@usm.my

**Abstract:** *The reactions of copper (II) acetate with thiourea, with or without chitosan, are described. The products obtained are CuS and Cu<sub>2</sub>S in an approximate composition of 1:1. UV-vis, Raman and FTIR spectroscopy as well as EDX analysis confirmed these copper sulfides. The effects of chitosan on the morphology of the copper sulfides were studied via TEM and SEM microscopy. In the absence of chitosan, fractal morphology was observed (D value 1.74). In the presence of chitosan, colloidal copper sulfides were obtained. For the colloid, an increase in chitosan concentration resulted in smaller copper sulfides particle size i.e. decreasing from 118.8 to 76.6 nm. A plausible mechanism of the copper sulfides formation via the involvement of ethanoate ions is also described.*

**Keywords:** chitosan, copper sulfide, thiourea, morphology, colloid

### 1. INTRODUCTION

The study of transition metal chalcogenides as nanomaterials has come under intense scrutiny by material scientists recently. Of the transition metal chalcogenides, sulfides and selenides have drawn considerable attention due to their interesting and excellent chemical and physical properties.<sup>1,2</sup> Transition metal sulfides have numerous applications in various fields. Some transition metal sulfides are highly refractory, with melting points exceeding those of oxides, and are stable during thin film formation by vacuum deposition. Most of these sulfides are crystalline and exhibit high lubricities. These features make these sulfides a far better photo-luminescent material as compared to oxides.<sup>3</sup> Many sulfides exhibit semi-metallic behaviour with respect to the ability to form multiple oxidation states, thus they are applicable in microelectronics as semiconductor materials.<sup>1,4</sup> For example, zinc and cadmium sulfides have been used in cathode ray tubes, while strontium sulfide is applied in the conversion of infrared radiation to visible light. Their quantum and charge transfer behaviour also contribute much to the photonics and catalyst industries.<sup>5,6</sup>

Among the transition metal sulfides that are widely studied include copper sulfides. Copper sulfides exist in various stoichiometries such as CuS and Cu<sub>2</sub>S at room temperature. Green copper sulfide or covellite, CuS is of particular interest to the industry as it exhibits a metal-like electrical conductivity.<sup>7</sup> Copper sulfides are also widely applied in thin films and composite materials for their unique properties such as opto-electronic,<sup>8</sup> high capacitance,<sup>9</sup> catalytic,<sup>6</sup> gas sensing,<sup>10</sup> etc. Apart from elemental sulphur,<sup>10</sup> different sulfur containing reagents have also been utilized as sulfur source. These include sodium sulfide, ammonium sulfide,<sup>11</sup> sodium thiosulfate,<sup>12</sup> thioacetamide,<sup>13</sup> as well as thiourea.<sup>14,15</sup> Among these sulfide donors, thiourea is widely applied in the formation of copper sulfides. For example, Gorai et al.<sup>8,16</sup> successfully synthesized a series of stoichiometric and non-stoichiometric copper sulfides via the solvothermal route using thiourea as a sulfur source. Besides being a sulfur source, thiourea can also act as a reducing agent.<sup>17</sup> Numerous attempts of synthesizing and characterizing copper sulfides nanoparticles have been reported. Sonochemical,<sup>18</sup> chemical bath deposition (CBD),<sup>19</sup> hydrothermal,<sup>12</sup> solvothermal,<sup>8</sup> and photochemical deposition<sup>20</sup> methods have been successfully employed. Lately, preparation of polymer-stabilized metal sulfides nanoparticles with the usage of polyaniline (PA),<sup>17</sup> poly(vinyl-alcohol) (PVA),<sup>11,18</sup> polyethyleneglycol (PEG) and polyvinylpyrrolidone (PVP)<sup>4</sup> have been reported. Among the advantages of preparing the polymer-stabilized nanoparticles is the ability to control particle size, enhance particle's stability and consistent morphology.

Being a naturally derived polymer, there is much interest to study the utilization of chitosan in the preparation of advanced materials. Chitosan has been studied as a protective polymer for gold nanocomposites,<sup>21</sup> platinum and palladium nanoparticles.<sup>22</sup> Reports on studies using chitosan as both reducing and protecting agent for the synthesis of gold nanoparticles have also been published.<sup>23</sup> Thus far, there has been no report on the synthesis of chitosan-stabilized copper sulfides. This article describes the preparation of colloidal chitosan-stabilized copper sulfides via chemical route employing thiourea as the sulfur source.

## **2. EXPERIMENTAL PROCEDURE**

### **2.1 Materials and Equipments**

The following commercially obtained materials were used without further purification: Chitosan of medium molecular weight  $\sim 400,000$  (Fluka, Switzerland), acetic acid 99.8%, copper acetate (both from BDH Chemicals, England), thiourea (Laboratory Chemicals Company).

The formation of copper sulfides nanoparticles was monitored using a HITACHI U2000 UV-vis spectrophotometer. The sample solutions taken at 30 min intervals, was cooled to room temperature prior to UV analyses. The FTIR spectra were recorded using a Thermo Nicolet IR200 spectrometer. The dried sample grounded with KBr and made into a pellet, was scanned from 400 to  $4000\text{ cm}^{-1}$  wavelength region. The size and morphology of the copper sulfides nanoparticles were obtained using a Philip CM 12 transmission electron microscope (TEM) operating at 80 kV. A drop of colloidal sample was carefully placed on a carbon coated copper grid and the solvent was evaporated off. The particles diameters were measured using a computer program "analySIS Docu 2.11" (GmbH, Germany). The average particle size and size distribution were obtained from  $\sim 300$  particles. The SEM micrographs and EDX spectra were obtained on a Leo Supra 50VP Field Emission Scanning Electron Microscopy (FE-SEM) equipped with Oxford INCA400 energy dispersive x-ray microanalysis system.

### **2.2 Preparation of Colloidal Copper Sulfides With and Without Chitosan Stabilizer**

Colloidal copper sulfides were synthesized via modification of the method reported by Shen et al.<sup>15</sup> The various concentration of  $\text{Cu}^{2+}$ :chitosan ratios used and other sample mixture compositions prepared are as tabulated in Table 1. For instance, for  $\text{Cu}^{2+}$ :chitosan = 1:2, the preparation is as follow: 5.0 ml ( $2.0 \times 10^{-5}$  M) aqueous copper (II) acetate solution, 5.5 ml ( $2.0 \times 10^{-5}$  M) aqueous thiourea solution, and 2.0 ml ( $1.0 \times 10^{-4}$  M) chitosan solution in 1.5% v/v aqueous acetic acid were added into a three-necked round bottom flask equipped with a reflux condenser. This was followed by the addition of deionized water to make up 50 ml of final solution volume. The mixture was reflux (bath temperature 115–120°C) with vigorous stirring. For the sample without chitosan, a further 2.0 ml of 1.5% v/v aqueous acetic acid was added to replace the chitosan solution.

Table 1: Table of sample compositions prepared

Reflux conditions		Volume of reagents used (ml)		
Cu <sup>2+</sup> in 50 ml reflux volume	Ratio of Cu <sup>2+</sup> :chitosan	2.0 × 10 <sup>-5</sup> M of copper acetate	2.0 × 10 <sup>-5</sup> M of thiourea	1.0 × 10 <sup>-4</sup> M of chitosan
2.0 × 10 <sup>-6</sup> M	1:2	5.0	5.5	2.0
	1:10	5.0	5.5	10.0
	1:20	5.0	5.5	20.0
	Without chitosan	5.0	5.5	-

### 3. RESULTS AND DISCUSSION

#### 3.1 Characterization

Typical UV-visible absorption spectrum of the colloidal copper sulfide-chitosan solution is shown in Figure 1. For 1:2 ratio of Cu<sup>2+</sup>:chitosan, two significant absorbance are observed within the range of 350–1100 nm. The broad absorbance at near-IR region 900–1100 nm is known to be characteristic of the covellite, CuS,<sup>1,7</sup> whereas the absorbance at 475 nm is due to the chalcocite, Cu<sub>2</sub>S.<sup>24,25</sup> On prolonged refluxing, the general trend of the maximum absorbance is red shifted (i.e. to higher wavelengths) for Cu<sub>2</sub>S and blue shifted (i.e. to lower wavelengths) for CuS.

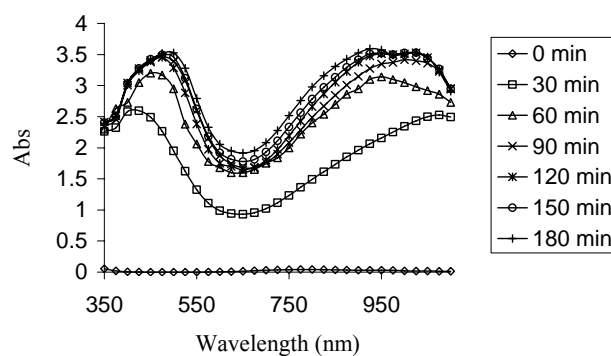


Figure 1: UV-vis absorptions of copper sulfides-chitosan colloids with respect to time of reaction

At different  $\text{Cu}^{2+}$ :chitosan ratios the characteristic absorbance of covellite and chalcocite show a gradual blue shifts from lower contents of chitosan to higher contents of chitosan. Figure 2 illustrates this effect for the formation of copper sulfides at 60 min. These shifts are most likely due to the decrease in particles size<sup>26</sup> and may be explained as due to the chitosan which contains amino-, hydroxyl- and ether functional groups that may be involved in and during the formation of copper sulfides. Chitosan can act as a reducing agent besides being a stabilizer or protecting agent.<sup>23</sup> So, it is understood that the presence of high contents of chitosan at reflux temperature will accelerate the formation of copper sulfides. Thus, smaller sized particles are produced at higher chitosan concentration.

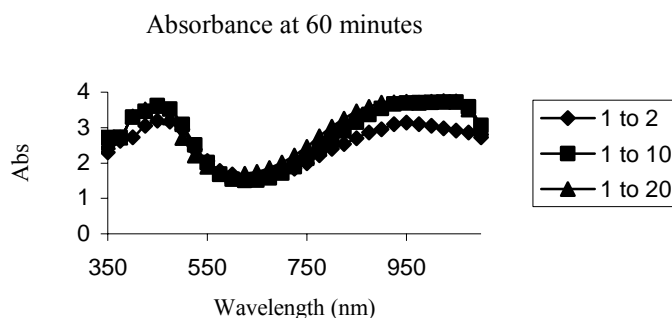


Figure 2: UV-vis absorption of various ratio of  $\text{Cu}^{2+}$ :chitosan at 60 min

Another significant observation is the increase and decrease in the maximum absorbance with time. This is depicted in Figure 3. The increase in absorbance as reaction time increases for reactions with chitosan as a stabilizer indicates that more copper sulfides nanoparticles are formed. However, without chitosan, during the early stages of the reaction time, the formation of the particles is indicated by the gradual increase in the UV-vis absorbance. These particles will eventually precipitate as the reaction progresses base on the decrease in absorbance. Visual inspections of the sample without chitosan confirm this phenomenon. The maximum absorbance of this colloidal solution is much lower than that of the chitosan stabilized colloids. Hence, the precipitation of the copper sulfides particles is attributed to the absence of chitosan as stabilizer.

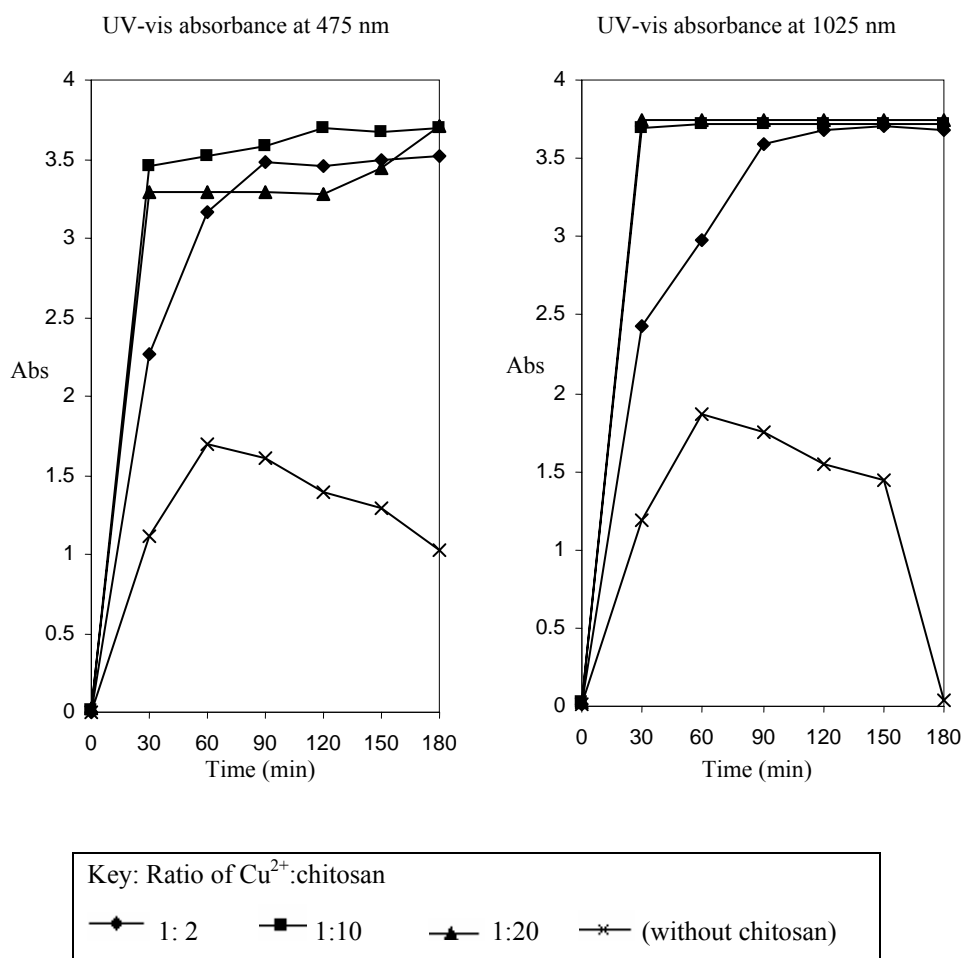


Figure 3: Evolution of UV-vis absorbencies ( $\lambda_{\text{max}}$ ) of (a)  $\text{Cu}_2\text{S}$  (475 nm) and (b)  $\text{CuS}$  (1025 nm)

Subsequently, the compositions and types in which the copper sulfides exist in the sample were determined using FTIR and Raman spectroscopy. The FTIR spectra of chitosan-stabilized copper sulfides at different ratios of  $\text{Cu}^{2+}$ :chitosan show similar features. A typical spectrum of chitosan-stabilized copper sulfides is shown in Figure 4(a). The chitosan spectrum, Figure 4(b), shows a shoulder at approximately  $1653\text{ cm}^{-1}$  which is assigned to the bending of N-H.<sup>27</sup> Comparison of the two spectra shows that this band shifts to lower wavenumbers at about  $1620\text{ cm}^{-1}$  in the chitosan-copper sulfides spectrum. It is inferred that the amine groups of chitosan adsorb on the surface of copper sulfides particles and stabilize the particles via amine-copper sulfides

interactions. Qi and Xu<sup>28</sup> reported a similar interaction between lead sulfide and chitosan. Two new bands at about 2918 and 619  $\text{cm}^{-1}$  are also seen in the chitosan-copper sulfides spectra. Dixit et al.<sup>24</sup> attributed these bands to the existence of  $\text{Cu}_2\text{S}$  in the product. Any band due to  $\text{CuS}$  is not observable in the IR spectra as the compound is not IR-active. Hence Raman spectroscopy was carried out to confirm the existence of  $\text{CuS}$ .

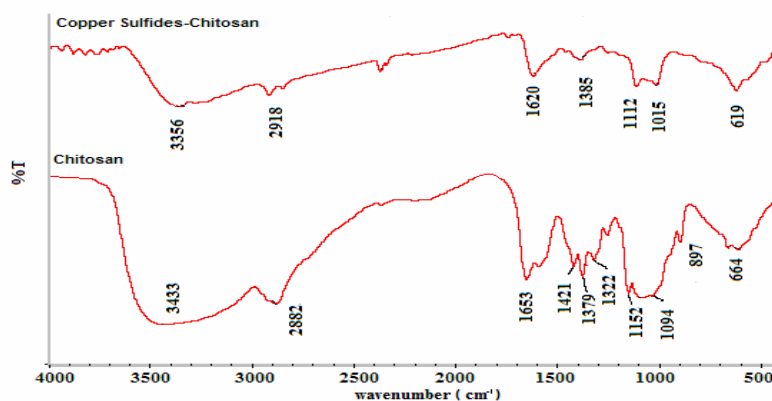


Figure 4: FTIR spectra of chitosan and typical chitosan-copper sulfides composite

Figure 5 shows the Raman spectrum of a typical sample. A sharp peak is observed at  $469 \text{ cm}^{-1}$  along with a smaller peak at  $265 \text{ cm}^{-1}$ . These peaks are indicative of the existence of  $\text{CuS}$ .<sup>29</sup> Hence, the existence of  $\text{Cu}_2\text{S}$  and  $\text{CuS}$  is confirmed by FTIR and Raman spectroscopy analysis, respectively. The result is in good agreement with the results obtained via UV-vis spectroscopy.

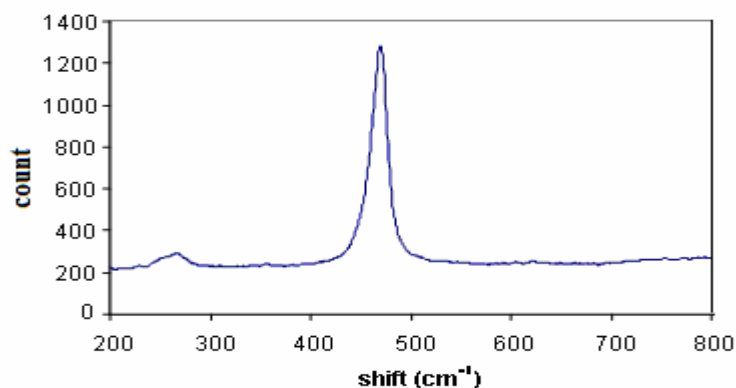


Figure 5: Raman spectrum of  $\text{CuS}$  nanoparticles

A typical EDX spectrum of the copper sulfides mixture is shown in Figure 6. The average elemental ratio of Cu:S calculated from the spectra is  $\sim 1.43$ . This result is closed to the value of 1.5, which indicates that the product composition is a mixture of covellite and chalcocite at an approximate ratio of 1:1.

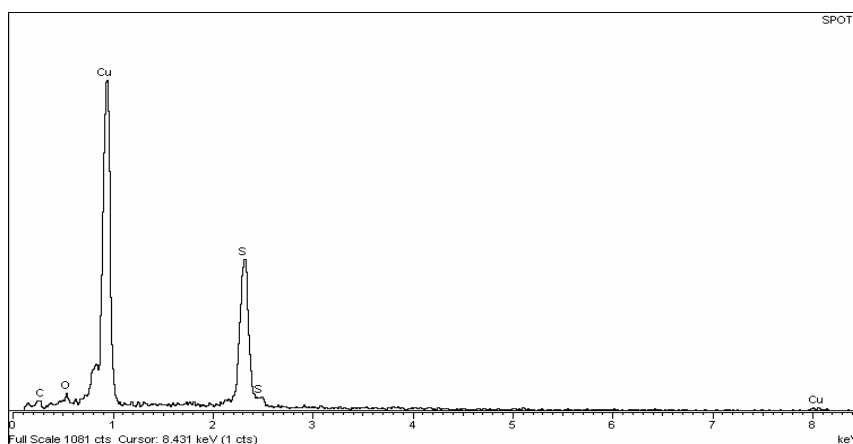


Figure 6: Typical EDX spectrum for copper sulfides mixture

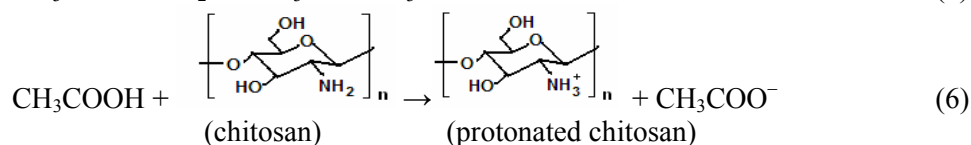
### 3.2 Mechanism of Formation

Dixit et al.<sup>24</sup> have synthesized a similar mixture of copper sulfides using copper-ammonia complex and thiourea. Based on their work, the formation of covellite, CuS can be described by the following equations:



From equations (2) and (3), it can be seen that the hydroxyl ions are responsible for generating the  $\text{S}^{2-}$  ions. However, in this work, hydroxyl ions are not generated but the active species is attributed to the ethanoate ions instead. Ethanoate ions are either generated by the dissociation of the acetic acid, equation (5) or upon protonation of chitosan by the acetic acid, equation (6). The ethanoate ions will react with thiourea [equation (7)] to generate  $\text{S}^{2-}$  ions and eventually combine with  $\text{Cu}^{2+}$  ions to form CuS according to equation (8).





In solution, copper (II) ions can readily be reduced to copper (I) ions by thiourea,<sup>17</sup> equation (9). The as-formed copper (I) ions then combine with sulfide ions to form chalcocite particles ( $\text{Cu}_2\text{S}$ ) as shown by equation (10). The availability of chitosan in the reaction solution stabilized the copper sulfides particles formed in equations (8) and (10).



Previous work has also shown that thiourea and chitosan can also form complex that is capable of stabilizing metal nanoparticles.<sup>30</sup> However, based on our FTIR results, thiourea-chitosan complexes are not observed. Hence, it can be summarized that the copper sulfides synthesized are stabilized only by the chitosan. Thiourea, on the other hand, acted as a source of sulfur atoms as well as a reducing agent.

### 3.3 Morphology

Figure 7 shows the TEM micrographs and size distributions of copper sulfides particles synthesized at different ratios of  $\text{Cu}^{2+}$ :chitosan. For 1:2 ratio of  $\text{Cu}^{2+}$ :chitosan, the particles formed are of irregular jagged spheres with an average size and size distribution of  $118.8 \pm 28.4$  nm. From the TEM images, all the particles are assembled close to each other but still distinguishable. Particles formed at 10:1 and 20:1 are of similar shape, but as the concentration of chitosan becomes higher, particles are more dispersed and the size becomes smaller with the average particle size and size distribution of  $116.1 \pm 25.8$  and  $76.5 \pm 29.0$  nm, respectively. This is due to steric hindrance caused by high concentration of chitosan, which impedes further growth of particles.<sup>31</sup> This observation is consistent with the UV-vis spectroscopic results.

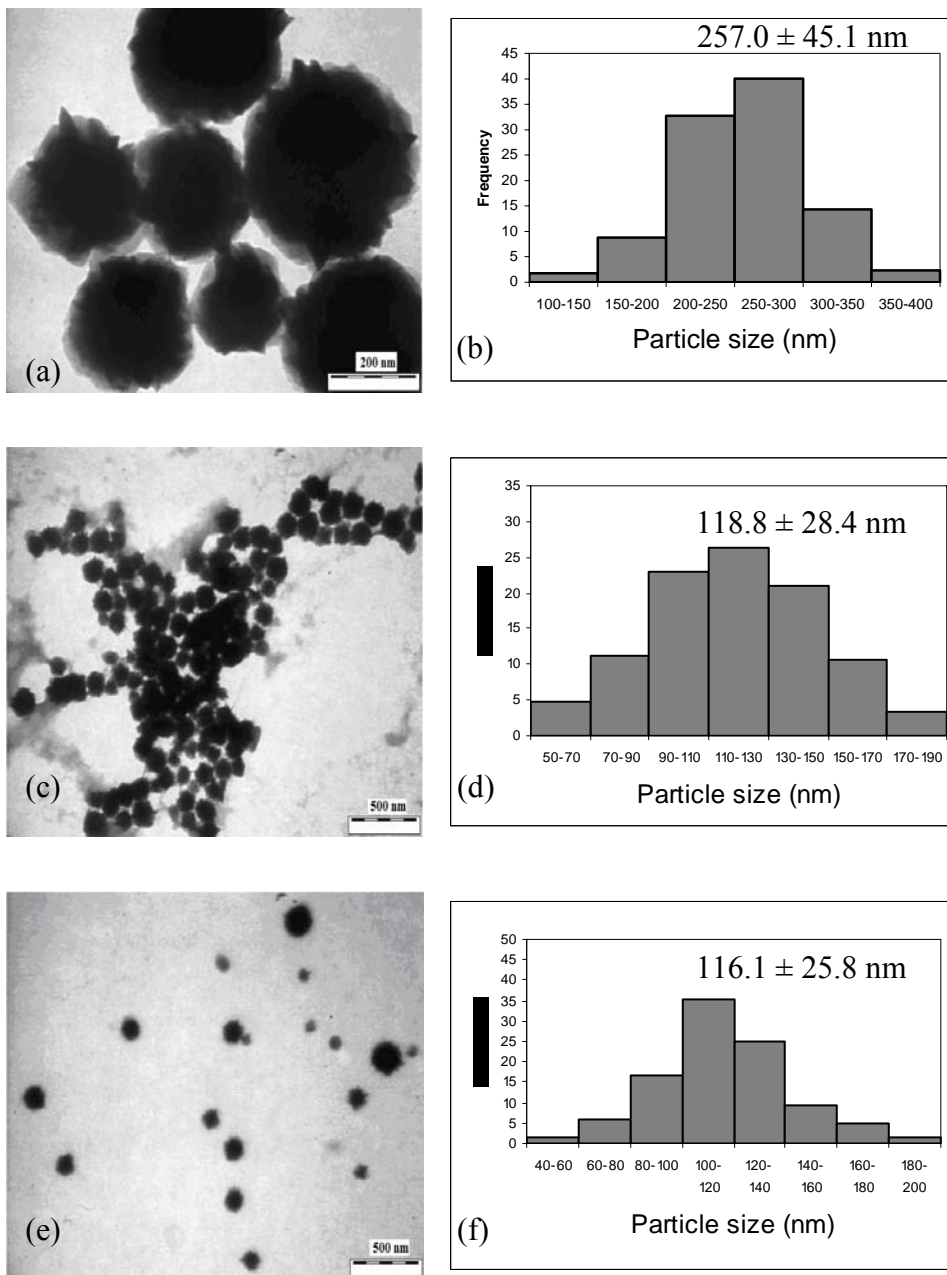


Figure 7: The respective TEM micrographs and size distributions for copper sulfides synthesized (a–b) without chitosan and at different ratio of  $\text{Cu}^{2+}$ :chitosan (c–d) 1:2, (e–f) 1:10, and (g–h) 1:20 (*continued*)

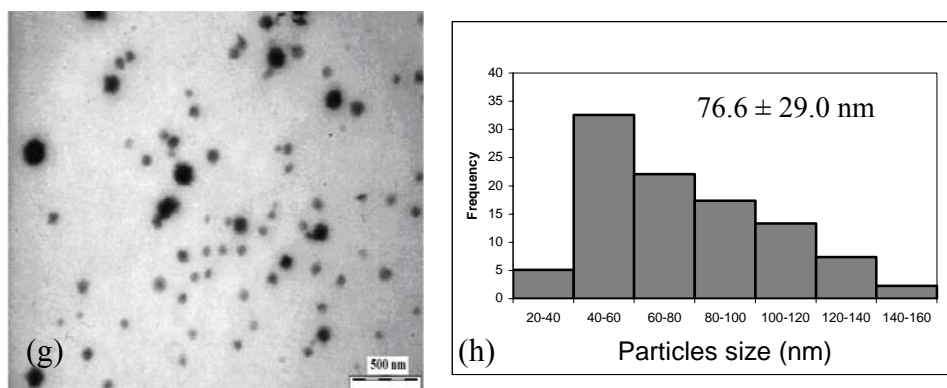


Figure 7: (continued)

In the absence of chitosan, the copper sulfides displayed a different morphology in that they tend to cluster together to form larger aggregates thus leading to fractal structures as shown in Figure 8(a). Fractal images are analysed using an optical microscopy method known as the box technique to calculate the fractal dimension,  $D$ .<sup>32</sup> This technique involves drawing a square in the center of fractal followed by a series of nested squares of increasing sizes,  $l$  (length of the box). Next, the micrograph is manually digitized using "ones" and "blanks" which corresponds to the presence and absence of the particle. Then, the number,  $N$  (ones), of particles within each square of different sizes,  $l$ , are counted. The fractal dimension,  $D$  is obtained from the slope of the plot of  $\log_{10} N$  against  $\log_{10} l$ . Based on the plot as shown in Figure 8(b), the  $D$  value obtained is 1.74. Based on this value, the fractal in this sample grew according to the cluster-cluster aggregation model as described previously.<sup>33</sup>

For a better understanding of the morphology of the as-synthesis copper sulfides, SEM analysis was carried out. A typical SEM micrograph is as shown in Figure 9. The micrograph reveals that the copper sulfides are of flower-like particles. Each flower-like copper sulfide crystal is actually a built up of uniform aligned nanoflakes. Hence, all of the irregular jagged spheres as seen in the TEM images are networks of interconnected flakes in 1-D dimension.

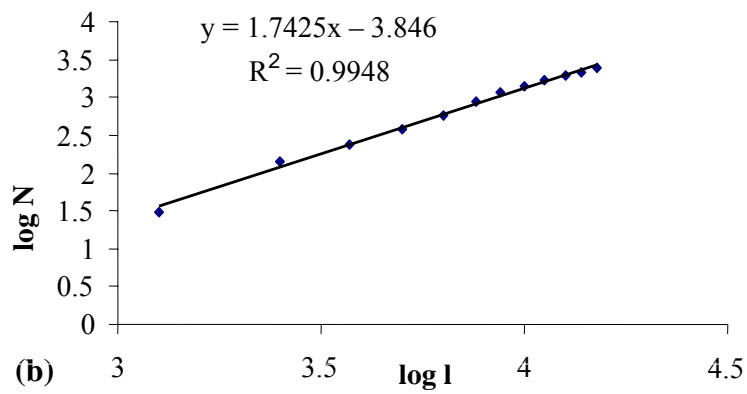
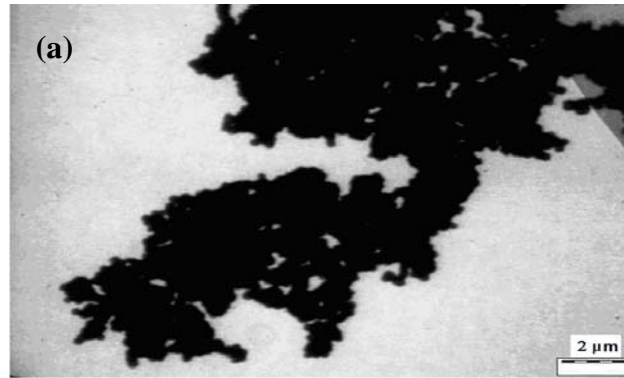


Figure 8: (a) TEM micrograph of copper sulfides exhibiting fractal structure and (b) a plot of  $\log_{10} N$  against  $\log_{10} l$

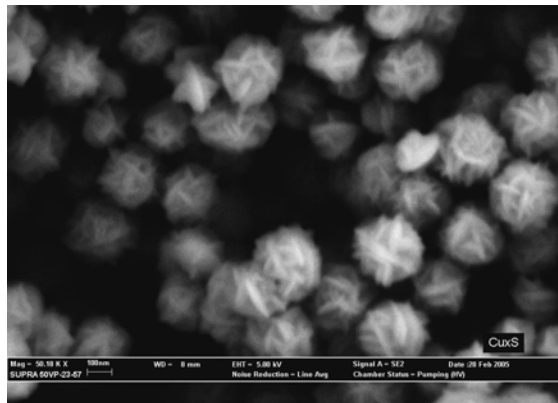


Figure 9: SEM micrograph of copper sulfides

#### 4. CONCLUSION

Mixtures of copper sulfides, CuS and Cu<sub>2</sub>S, stabilized with chitosan were synthesized using thiourea as a reducing agent as well as the sulfur source. The typical compositions of CuS and Cu<sub>2</sub>S mixture approximate 1:1. The copper sulfides appeared as irregular jagged spheres. In the absence of chitosan, fractal structures were formed, with average particles size and size distribution of  $257.0 \pm 45.1$  nm. These particles were unstable with respect to dispersion as evidence by precipitation after more than three hours of reaction time. However, stabilization can be improved by using chitosan. Various Cu<sup>2+</sup>:chitosan ratios were studied. Upon increasing the chitosan concentration, the average particle size of the copper sulfides particles decreased from 257.0 to 76.6 nm. Hence, chitosan plays a role in restricting the growth of the copper sulfides particles via the amine-copper interactions and therefore stabilized the copper sulfides colloids.

#### 5. ACKNOWLEDGEMENTS

The authors acknowledge the grant awarded by Universiti Sains Malaysia (FRGS 203/PKIMIA/670049) in support of this work.

#### 6. REFERENCES

1. Zhang, P. & Gao, L. (2003). Copper sulfide flakes and nanodiscs. *J. Mater. Chem.*, 13, 2007–2010.
2. Chen, X., Wang, Z., Wang, X., Zhang, R., Liu, X., Lin, W. & Qian, Y. (2004). Synthesis of novel copper sulfide hollow spheres generated from copper(II)-thiourea complex. *J. Cryst. Growth*, 263, 570–574.
3. Anonymous. *Technical Publication for Sulphides*. Retrieved 20 October 2004 from <http://www.cerac.com/pubs/proddata/sulphides.htm>.
4. Brelle, M.C., Torres-Martinez, C.L., McNulty, J.C., Mehra R.K. & Zhang, J.Z. (2000). Synthesis and characterization of Cu<sub>x</sub>S nanoparticles. Nature of the infrared band and charge-carrier dynamics. *Pure Appl. Chem.*, 72, 101–117.
5. Ding, T., Zhang, J., Long, S. & Zhu, J. (2003). Synthesis of HgS and PbS nanocrystals in a polyol solvent by microwave heating. *Microelectron. Eng.*, 66, 46–52.
6. Raevskaya, A.E., Stroyuk, A.L., Kuchmii, S.Y. & Kryukov, A.I. (2004). Catalytic activity of CuS nanoparticles in hydrosulfide ions air oxidation. *J. Mol. Catal. A: Chem.*, 212, 259–265.

7. Tan, C., Zhu, Y., Lu, R., Xue, P., Bao, C., Liu, X., Fei, Z. & Zhao, Y. (2005). Synthesis of copper sulfide nanotube in the hydrogel system. *Mater. Chem. Phys.*, 91, 44–47.
8. Gorai, S., Ganguli, D. & Chaudhuri, S. (2005). Shape selective solvothermal synthesis of copper sulphides: Role of ethylenediamine-water solvent system. *Mater. Sci. Eng. B*, 116, 221–225.
9. Chung, J.S. & Sohn, H.J. (2002). Electrochemical behaviors of CuS as a cathode material for lithium secondary batteries. *J. Power Sources*, 108, 226–231.
10. Balaz, P., Takacs, L., Boldizarova, E. & Godocikova, E. (2003). Mechanochemical transformations and reactivity in copper sulphides. *J. Phys. Chem. Solids*, 64, 1413–1417.
11. Lianos, P. & Thomas, J.K. (1987). Small CdS particles in inverted micelles. *J. Colloid Interface Sci.*, 117, 505–512.
12. Zhang, Y.C., Qiao, T. & Hu, X.Y. (2004). A simple hydrothermal route to nanocrystalline CuS. *J. Cryst. Growth*, 268, 64–70.
13. Liao, X., Chen, N., Xu, S., Yang, S. & Zhu, J. (2003). A microwave assisted heating method for the preparation of copper sulfide nanorods. *J. Cryst. Growth*, 252, 593–598.
14. Wang, Q., Xu, Z., Yin, H. & Nie, Q. (2005). Fabrication of transition metal sulfides nanocrystallites via an ethylenediamine assisted route. *Mater. Chem. Phys.*, 90, 73–77.
15. Shen, G., Chen, D., Tang, K., Liu, X., Huang, L. & Qian, Y. (2003). General synthesis of metal sulfides nanocrystallines via a simple polyol route. *J. Solid State Chem.*, 173, 232–235.
16. Gorai, S., Ganguli, D. & Chaudhuri, S. (2005). Synthesis of flower-like Cu<sub>2</sub>S dendrites via solvothermal route. *Mater. Lett.*, 59, 826–828.
17. Jagminas, A., Niaura, G., Judzentiene, A. & Juskenas, R. (2004). Spectroscopic evidence of a novel array AC fabrication within the alumina template pores from acidic Cu(II)-thiourea solution. *Appl. Surf. Sci.*, 239, 72–78.
18. Kumar, R.V., Palchik, O., Koltypin, Y., Diamant, Y. & Gedanken. (2002). Sonochemical synthesis and characterization of Ag<sub>2</sub>S/PVA and CuS/PVA nanocomposite. *Ultrason. Sonochem.*, 9, 65–70.
19. Khiew, P.S., Radiman, S., Huang, N.M. & Soot Ahmad, M. (2004). Synthesis and characterization of copper sulfide nanoparticles in hexagonal phase lyotropic liquid crystal. *J. Cryst. Growth*, 268, 227–237.
20. Podder, J., Kobayashi, R. & Ichimura, M. (2005). Photochemical deposition of Cu<sub>x</sub>S thin films from aqueous solutions. *Thin Solid Films*, 472, 71–75.
21. Esumi, K., Takei, N. & Yoshimura, T. (2003). Antioxidant-potentiality of gold-chitosan nanocomposites. *Colloids Surf. B: Biointerfaces*, 32, 117–123.

22. Adlim, M., Abu Bakar, M. & Ismail, J. (2004). Synthesis of chitosan-stabilized platinum and palladium nanoparticles and their hydrogenation activity. *J. Mol. Catal. A: Chem.*, 212, 141–149.
23. Huang, H. & Yang, X. (2004). Synthesis of polysaccharide-stabilized gold and silver nanoparticles: A green method. *Carbohydrate Res.*, 339, 2627–2631.
24. Dixit, S.G., Mahadeshwar, A.R. & Haram, S.K. (1998). Some aspects of the role of surfactants in the formation of nanoparticles. *Colloids Surf. A: Physicochem. Eng. Aspects*, 133, 69–75.
25. Haram, S.K., Mahadeshwar, A.R. & Dixit, S.G. (1996). Synthesis and characterization of copper sulfide nanoparticles in triton-X 100 water-in-oil microemulsions. *J. Phys. Chem.*, 100, 5868–5873.
26. Esumi, K., Hosoya, T., Suzuki, A. & Torigoe, K. (2000). Spontaneous formation of gold nanoparticles in aqueous solution of sugar-persubstituted poly(amidoamine)dendrimers. *Langmuir*, 16, 2978–2980.
27. Pavia, D.L., Lampman, G.M. & Kriz, G.S. (1996). *Introduction to spectroscopy* (2<sup>nd</sup> ed.). USA: Saunders College Publishing.
28. Qi, L. & Xu, Z. (2004). Lead sorption from aqueous solutions on chitosan nanoparticles. *Colloids Surf. A: Physicochem. Eng. Aspects*, 251, 183–190.
29. Munce, C.G., Parker, G.K., Holt, S.A. & Hope, G.A. (2007). A Raman spectroelectrochemical investigation of chemical bath deposited Cu<sub>x</sub>S thin film and their modification. *Colloids Surf. A: Physicochem. Eng. Aspects*, 295, 152–158.
30. Chen, S., Wu, G. & Zeng, H. (2005). Preparation of high antimicrobial activity thiourea chitosan-Ag<sup>+</sup> complex. *Carbohydrate Polym*, 60, 33–38.
31. Chastellain, M., Petri, A. & Hofmann, H. (2004). Particle size investigations of a multistep synthesis of PVA coated superparamagnetic nanoparticles. *J. Colloids Interface Sci.*, 278, 353–360.
32. Forrest, S.R. & Witten T.A. (1979). Long-range correlations in smoke-particle aggregates. *J. Phys. A: Math. Gen.*, 12, 109–117.
33. Vicsek, T. (1989). *Fractal growth phenomena*. Singapore: World Science Publishing, 209–264.